JOURNAL OF Materials CHEMISTRY

Investigation of the electronic properties of substituted $LaNi_5$ compounds used as material for batteries

V. Paul-Boncour,*[a] M. Gupta,[b] J.-M. Joubert,[a] A. Percheron-Guégan,[a] P. Parent[c] and C. Laffon[c]

[a]*Laboratoire de Chimie Métallurgique des Terres Rares, CNRS, GLVT, 2-8 rue Henri Dunant, F-94320 Thiais, France. E-mail: Valerie.Paul-boncour@glvt-cnrs.fr*
[b]*Institut des Sciences des Matériaux, bat 415, LEMHE, Université Paris Sud, F-91405 Orsay cedex, France*
[c]*LURE, bat 209D, UPS, F-91405 Orsay cedex, France*

Received 26th April 2000, Accepted 7th September 2000
First published as an Advance Article on the web 20th October 2000

The electronic properties of $LaNi_5$ and substituted $LaNi_4M$ (M = Mn, Fe, Co, Cu and Al) and $LaNi_{3.55}Mn_{0.4}Al_{0.3}Co_{0.75}$ compounds have been studied by X-ray absorption (XAS) and photoemission (PES) spectroscopies in order to understand the influence of the substitutions on the electrochemical properties of these materials in rechargeable batteries. The experimental results are compared with band structure calculations. The valence band of $LaNi_5$ is dominated by the Ni 3d band. Ni substitution by another 3d metal leads to the formation of an additional 3d subband which is above that of Ni for Mn, Fe and Co and below for Cu, in agreement with density of states (DOS) calculations. Al substitution leads to a progressive filling of the Ni d band associated with a decrease of the DOS at E_F. In $LaNi_{3.55}Mn_{0.4}Al_{0.3}Co_{0.75}$ (LaNi3S), the XAS measurements indicate that the filling of the individual 3d subbands is different from the corresponding ones in $LaNi_4M$ single substituted compounds (M = Mn and Co). The total number of holes in the d bands of the transition elements of the LaNi3S compound is found to be the same as in $LaNi_4Co$. The complete filling of these states by 4 H atoms per formula unit in $LaNi_4CoH_4$ as well as in the LaNi3S hydride is associated with a particular stability of the compounds up to this hydrogen concentration, a feature which has been observed in the pressure–composition isotherms and which appears to play an important role in the longer cycle life of these electrode materials.

I Introduction

Intermetallic compounds of the $LaNi_5$ type form reversible hydrides either by solid–gas or by electrochemical reaction. They are now widely used as negative electrodes in rechargeable Ni-metal hydrides (Ni-MH) batteries.[1] The hydrogen equilibrium pressure of $LaNi_5$ is above 1 bar at room temperature and is too high to obtain the maximum capacity of 6 hydrogens per formula unit [H (f.u.)$^{-1}$] or 370 mA h g^{-1} for the electrochemical charge in an open cell. Partial Al and Mn substitution for nickel allow the equilibrium pressure to be decreased and therefore improve the initial capacity of the electrode,[1] but not the cycle life related to the corrosion process. In contrast, the substitution of cobalt for nickel induces only a small decrease of the equilibrium pressure but improves significantly the cycle life of the electrode.[2,3] Very good electrochemical performances were finally obtained for the multicomponent compound $MmNi_{3.55}Mn_{0.4}Al_{0.3}Co_{0.75}$ (Mm = Mischmetal), which exhibits a strong resistance to corrosion and therefore a long cycle life.[4,5] However Co is very expensive, and represents 40% of the price of the alloy. In order to reduce the cost of the batteries, several crystallographic, thermodynamic, electrochemical and kinetic studies have been performed to determine the role of each substituted element and especially that of Co in the multicomponent compound compared to the $LaNi_{5-x}M_x$ (M = Al, Mn, Co) single substituted compounds.[6,7] Thermodynamic studies have shown that the multicomponent compound displays a shorter pressure plateau, which corresponds to a mixture of hydrogen solid solution in the metal (α phase) and hydride (β phase), up to about 4 H (f.u.)$^{-1}$ and a larger range of hydrogen solid solution in the hydride up to 5.5 H (f.u.)$^{-1}$ (β branch) compared to those obtained for the single substituted compounds. *In situ* neutron diffraction studies[7] have shown that the electrode of the multicomponent compound works mainly in the β branch, limiting the α↔β transformation, and thus reducing the large volume change ($\Delta V/V$) which is responsible for the rapid corrosion by renewing the surface of the metal and hydride grains on cycling. This large increase of volume leads also to a decrease of the electrochemical capacity due to a loss of electrical contact between the grains.[6] The origin of this large β branch may be due to the presence of cobalt, since the $LaNi_{5-x}Co_x$–H_2 systems display two plateaux with the formation of an intermediate hydride for about 4 H (f.u.)$^{-1}$.[8,9] The existence of intermediate hydrides or large range solid solution may be explained by the electronic properties of the intermetallic compounds and their hydrides.

Electronic properties, in particular band filling effects, play an important role in the stability (heat of formation) of the intermetallic compounds and of their hydrogen capacity.[10] Specific heat measurements showed a relationship between the amount of stored hydrogen and the number of holes in the conduction band, *i.e.* the filling of the conduction band by alloying effects decreases significantly the hydride capacity.[11]

Photoemission (PES) and X ray absorption (XAS) spectroscopies have been used in previous years to study the modifications of the electronic structure of metallic matrices upon hydrogen absorption.[10] More recently, PES[12] and *in situ* XAS[13–15] have been applied to study metal hydride electrodes of the $LaNi_5$ family, and have shown the existence of large electronic and structural changes upon hydrogen absorption.

In the present work, in order to gain a better understanding

of the influence of Ni substitution by one or several elements, we have studied the electronic properties of the $LaNi_4M$ (M = Al, Mn, Fe, Co, Ni, and Cu) and $LaNi_{3.55}Mn_{0.4}Al_{0.3}Co_{0.75}$ (LaNi3S) intermetallic compounds by XAS and PES in conjunction with density of states (DOS) calculations. A multicomponent compound with lanthanum rather than with mischmetal, used to reduce the cost of the electrode, was chosen in order to compare its experimental results with the $LaNi_4M$ based compounds and to band structure calculations.

XAS at the L_{II-III} edge of the transition metal probes the density of unoccupied d states which is the main contribution above the Fermi level in these compounds. It was used recently to study the d-electron charge transfer in Ni–Cu alloys.[16] PES experiments were also performed to measure the valence band and the Ni 3p photoemission lines in these compounds.

Although it is desirable to include many body effects and matrix elements to provide detailed interpretation of PES and especially XAS spectra since the latter are strongly influenced by core hole effects, such elaborate calculations are not available to date for the complex systems under study. We will thus interpret the experimental results, as currently found in the literature,[17] by means of band structure calculations performed on $LaNi_5$, $LaNi_4M$ and $LaNi_{3.5}Al_{0.25}Mn_{0.5}Co_{0.75}$ compounds, an account of which has been reported in ref. 18.

II Sample preparation and experimental conditions

The intermetallic compounds were prepared by induction melting of the pure components (La 99.9%; Mn, Fe, Co, Ni, Cu, Al 99.99%) in a water-cooled copper crucible under an He atmosphere (99.9995%). The temperature of melting was higher than 1350 °C. The ingots were annealed at appropriate temperatures (see Table 1) under low He pressure before quenching to obtain single phase and homogeneous samples. The homogeneity and the stoichiometry of the alloys were checked by metallographic examination and electron probe microanalysis (EPMA) with a Camebax datanim apparatus. The X-ray diffraction (XRD) patterns were measured with a Philips PW1170 diffractometer using Cu K_α radiation. All the samples were single phase and their XRD patterns were refined in the $CaCu_5$-type hexagonal cell of $LaNi_5$. The composition of the samples measured by EPMA and the cell parameters are given in Table 1. The cell parameters and the cell volumes of the intermetallic compounds are in agreement with the values previously published.[6,19]

The experiments were performed on the SA22 line with the SUPERACO ring (LURE, Orsay) on the SACEMOR apparatus using a high energy SM-PGM monochromator. The XAS spectra were recorded in partial electron yield and the photoemission measurements at 200 eV using a CLAM2 (VG) analyser with a total resolution of 0.3 eV. This experiment allows both XAS and PES spectra to be measured on the same sample zone.

The samples were slices with a surface of about 1 cm^2 and a thickness of 2 to 4 mm, which were cut from the ingots and polished to obtain parallel faces. Each sample was fixed on a sample holder, introduced in the preparation chamber, and evacuated under high vacuum (10^{-8} Torr) during several hours. Two methods were tested to clean the surface of the sample, either mechanically with a diamond file or by Ar^+ sputtering, before transferring the sample into the analysis chamber (10^{-10} Torr). Both methods allowed the amount of oxygen to be reduced markedly, measured at the O-K edge, but the Ar^+ sputtering led also to an amorphization of the surface of the sample. The mechanical cleaning was therefore selected to prepare all the samples. After this treatment, the amount of oxygen was small and almost the same for all the samples except for $LaNi_4Al$, for which it was 1.5 times larger. A single crystal of Ni(111) was used as the reference compound.

III Computational details

The band structure calculations were performed using the density functional theory (DFT) in the local density approximation. The von Barth–Hedin[20] approach was used to determine the exchange and correlation terms of the crystal potential. Since we are dealing with unit cells containing a rather large number of atoms, we used the self-consistent linear muffin-tin orbital (LMTO) method within the atomic sphere approximation (ASA).[21] The so-called combined correction terms were included to account for the overlap of atomic spheres. The densities of states (DOS), as well as their sites and partial wave analysis up to $l = 3$, were calculated in a 1 mRy mesh with the linear energy tetrahedron method.[22]

$LaNi_5$ crystallises in the hexagonal $CaCu_5$ structure, space group *P6/mmm*, in which the La atoms occupy the 1a site; there are two types of Ni atoms occupying respectively the 2c sites in the basal lanthanum planes ($z = 0$), and the 3g sites in the middle plane ($z = 1/2$). Neutron scattering data[23,24] have shown that the Ni substitutions considered here occur predominantly at the Ni 3g sites. For simplicity we therefore ignored the partial, and generally small, occupancy of the 2c sites as well as the disorder and the possible clustering of the substituting elements by assuming an ordered array of the M atoms. On the other hand, in the case of $LaNi_4Co$ we also considered the Co substitution at the 2c site, since it is not negligible. The calculations were performed for a trisubstituted compound $LaNi_{3.5}Mn_{0.5}Al_{0.25}Co_{0.75}$ of composition close to that of the experimental sample ($LaNi_{3.55}Mn_{0.4}Al_{0.3}Co_{0.75}$), using a supercell containing four formula units.

IV Experimental results

IV-A X-Ray absorption

The Ni $L_{II,III}$ edges of $LaNi_5$ are very similar to those of pure Ni metal as seen in Fig. 1 and this is observed despite the fact that in $LaNi_5$ the La M_{IV} edge partially overlaps the Ni L_{III} edge. The La M_{IV} and Ni $L_{II,III}$ edges of $LaNi_5$, $LaNi_4M$ and LaNi3S compounds are shown in Fig. 2. The $M_{IV,V}$ edges which correspond to the transition $3d^{10}4f^0 \rightarrow 3d^9 4f^1$ are not very sensitive to the chemical bonding, since the 4f states are strongly localised. It was therefore assumed that the La $M_{IV,V}$

Table 1 Annealing temperatures, cell parameters, cell volume, *c/a* ratio and electron probe microanalysis (EPMA) of the intermetallic compounds. The standard deviation of the cell parameters is ±0.001 Å

Compound	Annealing temperature/°C	*a*/Å	*c*/Å	*V*/Å^3	*c/a*	EPMA
$LaNi_5$	1100	5.017	3.981	86.78	0.794	
$LaNi_4Co$	1100	5.031	3.984	87.33	0.792	$La_{1.07(2)}Ni_{4.02(3)}Co_{0.97(3)}$
$LaNi_4Cu$	800	5.040	4.009	88.19	0.795	$La_{1.00}Ni_{4.02}Cu_{0.98}$
$LaNi_4Fe$	1080	5.053	4.020	88.89	0.796	$La_{1.01}Ni_{4.02}Fe_{0.97}$
$LaNi_4Mn$	900	5.091	4.060	91.13	0.798	$La_{1.02}Ni_{4.06}Mn_{0.92}$
$LaNi_4Al$	900	5.070	4.076	90.74	0.804	$La_{1.03}Ni_{4.05}Al_{0.92}$
LaNi_3S	900	5.072	4.046	90.14	0.798	$La_{1.01}Ni_{3.58}Mn_{0.41}Al_{0.27}Co_{0.74}$

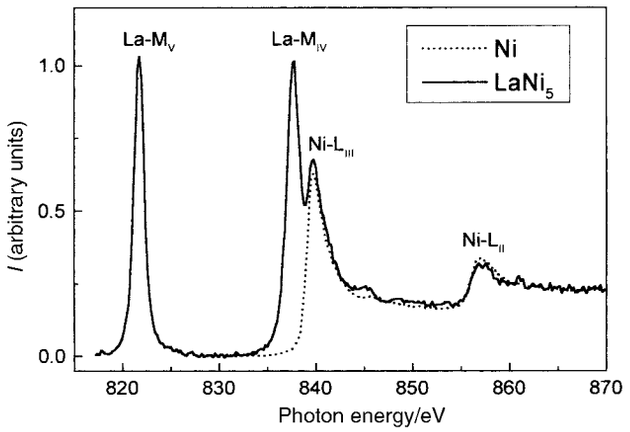

Fig. 1 The La M_{IV-V} and Ni L_{II-III} edges of $LaNi_5$ and the Ni L_{II-III} edge of Ni.

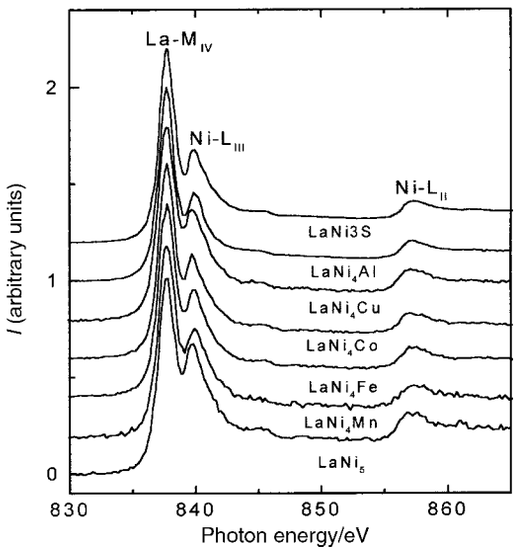

Fig. 2 The La M_{IV} and Ni L_{II-III} edges of $LaNi_4M$ and $LaNi_{3.55}Al_{0.3}Mn_{0.4}Co_{0.75}$ (LaNi3S).

edges remain unchanged for all the $LaNi_5$ based compounds and the La M_{IV} edge (837 eV) was used to calibrate in energy the spectra in Fig. 2. The intensities of the spectra were normalised to one at the maximum of the La M_{IV} edge at 837 eV.

The main effect is a decrease of the Ni L_{II-III} intensities in the substituted compounds compared to that of $LaNi_5$ (Fig. 2). This decrease is in agreement with the stoichiometry of the bulk intermetallic compounds: compared to $LaNi_5$ the relative Ni intensity is 4/5 for the $LaNi_4M$ compounds (M = Mn, Fe, Co and Cu) and 3.5/5 for LaNi3S. For $LaNi_4Al$ the Ni intensity is close to 3.5/5 instead of 4/5.

The Ni L_{II} edges of Ni, $LaNi_5$, $LaNi_4M$ and LaNi3S compounds were normalised to one after the absorption edge and are detailed in Fig. 3. For all the compounds in addition to the white line, a satellite is observed at 6 eV above the edge. The energy differences between the Ni L_{II} absorption edges of these compounds are weak, and remain in the range of the instrumental errors.

The L_{II} and L_{III} edges of Ni in pure Ni and of the transition element in the $LaNi_4M$ substituted compounds (M = Mn, Fe, Co and Cu) are presented in Fig. 4. They are in agreement with those published earlier for pure transition metals[25] showing that for all the samples the transition metals are in the metallic state and not oxidized. As the atomic number increases from Mn to Cu, the difference in energy between the L_{II} and the L_{III}

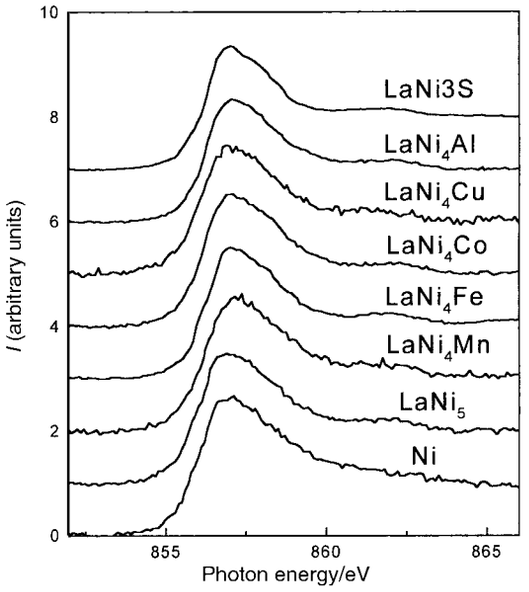

Fig. 3 The Ni L_{II} edges of Ni, $LaNi_5$, $LaNi_4M$ and LaNi3S.

edge increases, whereas the white line intensity of both edges decreases. Since the number of 3d electron increases from Mn to Cu, the probability to excite an electron from the 2p level to an empty d state decreases. The collapse of the white line from Mn to Cu reflects the progressive filling of this d band.

Concerning LaNi3S the normalised Mn and Co L_{II-III} edges are compared to those of $LaNi_4Mn$ and $LaNi_4Co$ in Fig. 5. At the Mn L_{II-III} edge the white line intensity of the LaNi3S compound increases compared to that of $LaNi_4Mn$ whereas the opposite is observed at the Co L_{II-III} edge. This change of the white line intensity between single and trisubstituted compounds indicates that the density of the empty Mn and Co d states is modified: the Mn d band should be less filled and the Co d band more filled in the LaNi3S compound.

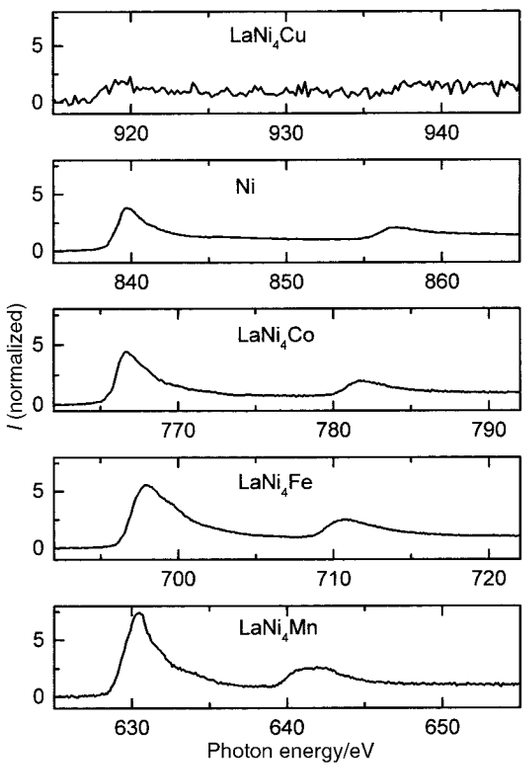

Fig. 4 L_{II-III} transition metal edges in pure Ni and $LaNi_4M$ (M = Mn, Fe, Co and Cu).

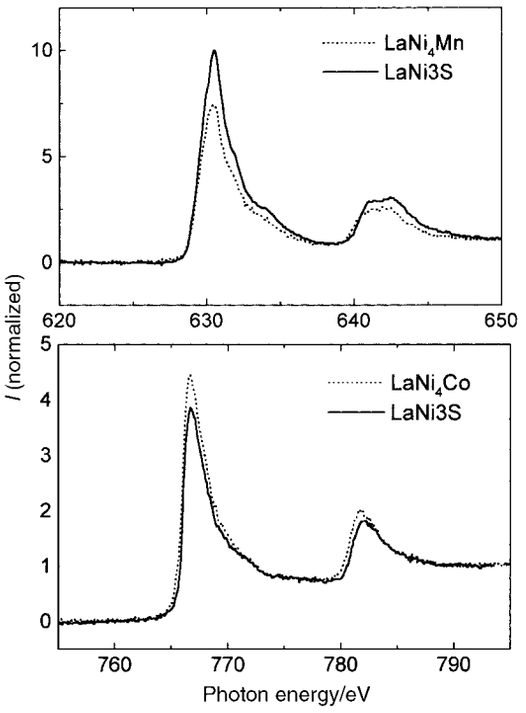

Fig. 5 Mn L_{II-III} edges of $LaNi_4Mn$ and LaNi3S (top) and Co L_{II-III} edges of $LaNi_4Co$ and LaNi3S (bottom).

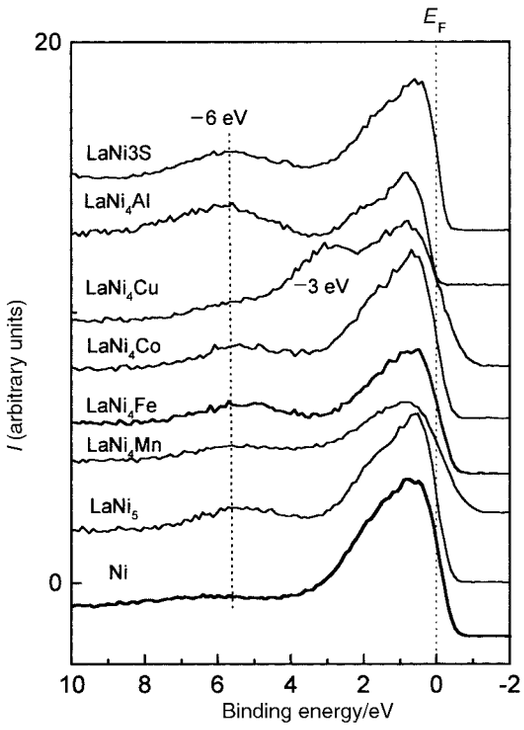

Fig. 6 Valence bands of the Ni, $LaNi_4M$ (M = Mn, Fe, Co, Ni, Cu, Al) and LaNi3S intermetallic compounds. E_F indicates the origin of energies.

IV-B Photoemission

The Ni 3p photoemission peaks at 67 eV of $LaNi_5$ (not shown here) and of the $LaNi_4M$ compounds are similar to those of pure Ni metal. Since no chemical shift was observed at the Ni L_{II-III} edge of the compounds, nor in the Ni 3s spectra of Ni–Cu alloys,[16] it was assumed that the Ni substitution by another element did not lead to significant chemical shifts in the Ni 3p spectra. These Ni 3p peaks were therefore used to calibrate the binding energy and to normalize the intensity of the valence bands in the intermetallic compounds, taking into account the amount of Ni in each sample.

The valence band of $LaNi_5$ is compared in Fig. 6 to that of the Ni(111) single crystal. The Fermi level is located at the same position, and the width of the contribution near the Fermi level is the same. The shapes of the valence bands of the $LaNi_4M$ compounds, presented in Fig. 6, vary strongly as a function of the substituted transition element.

For $LaNi_4Mn$ the valence band is wider and displays a lower intensity than in $LaNi_5$. For $LaNi_4Fe$ the intensity at the Fermi level is also lower than in $LaNi_5$. For $LaNi_4Co$, the valence band is very similar to that of $LaNi_5$. For $LaNi_4Cu$, larger changes are observed: the intensity of the peak at the Fermi level slightly decreases, a new peak appears at 3 eV below E_F. The presence of an additional contribution in the valence band of $LaNi_{5-x}Cu_x$ intermetallic compounds compared to $LaNi_5$ has been observed[26] at the same binding energy. For $LaNi_4Al$, the density of states at E_F is much lower than in $LaNi_5$. The valence band of LaNi3S is not very different from that of $LaNi_5$: only a small decrease of the peak intensity at the Fermi level is visible. In all the samples a structure is also observed at about 6 eV below E_F. Weinelt *et al.*[27] and Fuggle *et al.*[28] have explained this satellite by the contribution of a d^8 final state configuration in Ni in relation to the unfilled Ni d band.

In the spectra of Fig. 6, some variations of the satellite intensities are observed. According to the previous interpretation a decrease of the satellite intensity should correspond to the filling of the Ni d band. Small additional contributions due to lanthanum oxide or hydroxide at the surface may also contribute to the spectra in the same energy range as the satellite. However, such oxide contamination does not extend over the metal d band, as shown by the photoemission spectra recorded on an unscraped sample of the series (not presented here). Therefore, we will not discuss further this satellite contribution and the discussion will be focused on the shape of the d bands near the Fermi level.

V Discussion of the experimental and theoretical results

The valence band measured for $LaNi_5$ is close to that obtained for pure Ni, in agreement with previous photoemission work of Fuggle *et al.*[28] This is due to the fact that the density of the occupied states of $LaNi_5$ is dominated by the Ni d band, which is not completely filled as shown by DOS calculations plotted in Fig. 7. The 5d states of La are hybridised with the 3d states of Ni, but their contribution to the DOS at the Fermi energy, E_F, is only 4%. The main contribution of the 5d states of La is

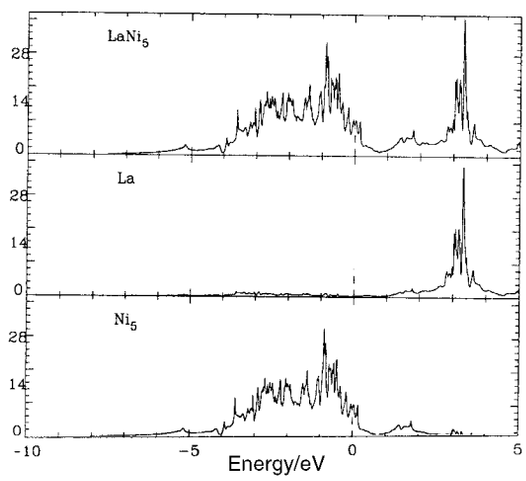

Fig. 7 The total density of states of $LaNi_5$ (top panel) and its components at the atomic sites. Units are states of both spin per eV. The Fermi energy is chosen at the origin of energies.

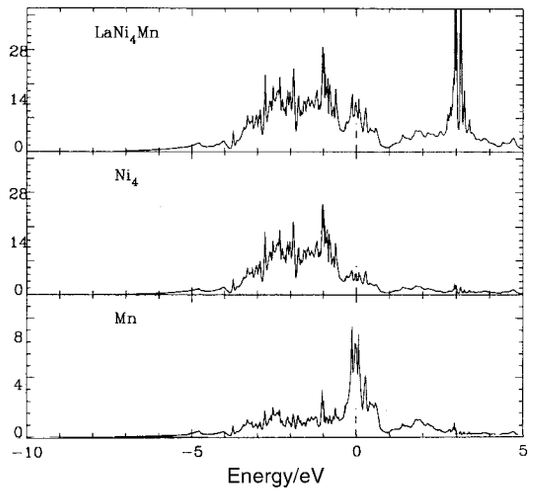

Fig. 8 The total density of states of $LaNi_4Mn$ (top panel) and its components at the atomic sites. Units are states of both spin per eV. The Fermi energy is chosen at the origin of energies.

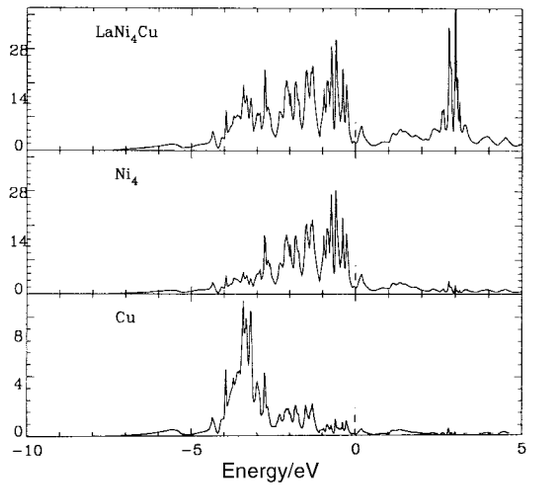

Fig. 10 The total density of states of $LaNi_4Cu$ (top panel) and its components at the atomic sites. Units are states of both spin per eV. The Fermi energy is chosen at the origin of energies.

located above E_F; the La 4f states are unoccupied and they give rise to the sharp peak in the DOS around 3 eV above E_F. Owing to partial filling of the Ni s,p states, the number of holes in the Ni d bands of pure f.c.c. nickel is of the order of 0.6, leading to 3 holes in Ni_5. If the Ni d bands were not hybridised with the La 5d states in $LaNi_5$, and since they are located at lower energy, one would expect complete filling of the 3 holes in the Ni states of $LaNi_5$ by transfer of the 3 conduction electrons of La. The photoemission spectrum as well as the theoretical results show clearly that this is not the case and thus $LaNi_5$ is not a charge transfer compound. As shown in Fig. 7, the contribution of the La d,s,p states below E_F, although small compared to that of the Ni states, is non-negligible.

Let us discuss the influence of nickel substitution by another 3d element (Mn, Fe and Co). The densities of states calculated for $LaNi_4M$ (M = Mn, Co) are plotted in Fig. 8 and 9 respectively. We can see that the substitution leads to the formation of a new narrow d subband of the substituted transition element, located above the d Ni band. This subband is located 0.5 eV above that of Ni for the Mn compound, and becomes closer for Fe[18] and Co. In addition, the Fermi level E_F falls in this new d subband. Indeed, for $LaNi_4Mn$, the experimental valence band widens around the Fermi level compared to that of nickel. For $LaNi_4Fe$ the band broadening becomes smaller and for $LaNi_4Co$ it cannot be detected experimentally. This means that the narrow subband cannot be completely resolved in the PES valence band when it becomes closer to the Ni subband. The instrumental resolution (photons and electrons) was 0.3 eV and the lifetime of the final state should also be considered to explain the width of the valence band. The evolution of the experimental valence band intensity, which increases from Mn to Co, also reflects the modification of the d states distribution in the DOSs.

For $LaNi_4Cu$, the DOSs plotted in Fig. 10 indicate the presence of a new Cu subband located around 3 eV below the Fermi level which corresponds to the structure at 3 eV in the valence band photoemission spectrum of $LaNi_4Cu$ (Fig. 6). In addition, the Ni d band is shifted towards lower energies and the DOS at E_F decreases, as it is observed in the valence band of $LaNi_4Cu$. This is in agreement with the DOS calculation since a partial wave analysis indicates that around the Fermi energy the states have mostly s character and a vanishing d contribution at the copper site. This is not the case for the Ni L_{II-III} edge indicating, in agreement with the band structure calculations, that the Ni d band is not completely filled in this compound.

The DOSs of $LaNi_4Al$, plotted in Fig. 11, show a new structure between −6 and −8 eV due to the Al s states. The p states contribution becomes significant above −6 eV. Compared to $LaNi_5$, a large decrease of the DOS at

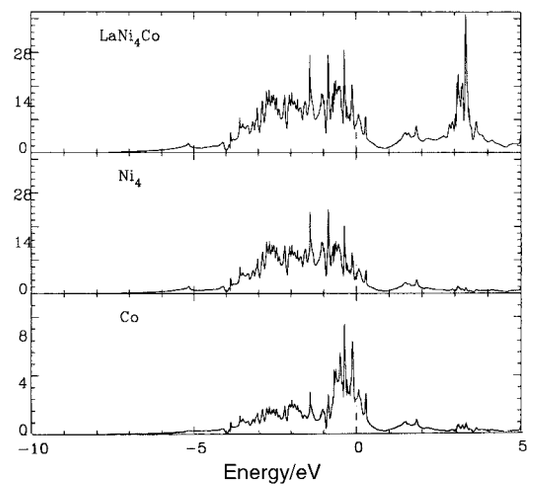

Fig. 9 The total density of states of $LaNi_4Co$ (top panel) and its components at the atomic sites. Units are states of both spin per eV. The Fermi energy is chosen at the origin of energies.

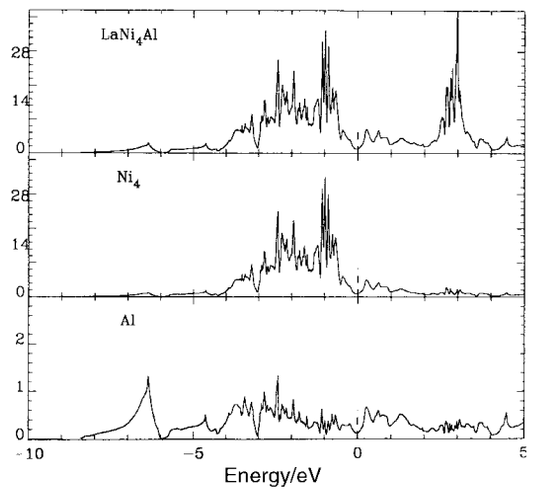

Fig. 11 The total density of states of $LaNi_4Al$ (top panel) and its components at the atomic sites. Units are states of both spin per eV. The Fermi energy is chosen at the origin of energies.

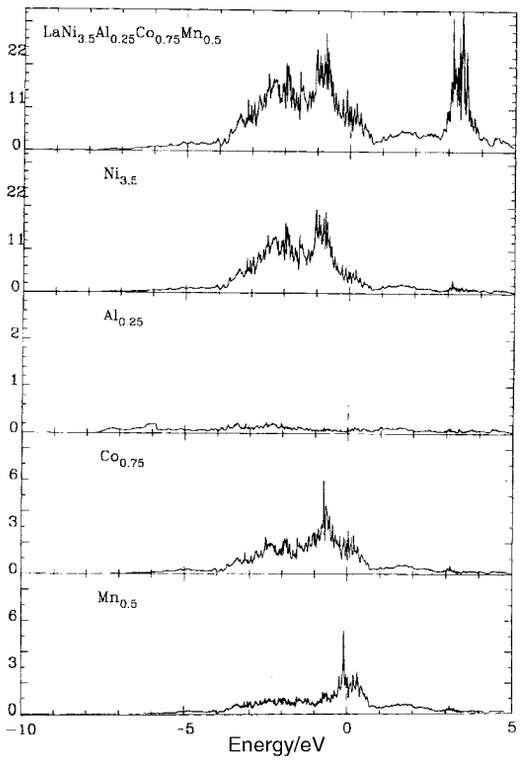

Fig. 12 The total density of states of $LaNi_{3.5}Al_{0.25}Co_{0.75}Mn_{0.5}$ (top panel) and its components at the atomic sites. Units are states of both spin per eV. The Fermi energy is chosen at the origin of energies.

E_F is observed, since E_F is located in the valley between the Ni d states and the La d states. The experimental decrease of the valence band intensity at E_F for $LaNi_4Al$ compared to that of $LaNi_5$ is in agreement with the DOS calculation. The increase of the satellite intensity at -6 eV compared to that of $LaNi_5$ cannot be explained as final Ni d^8 states, since it should decrease due to the filling of the Ni d band. This means that other contributions like the Al s states, located at -6 eV below E_F and maybe some aluminium oxide have to be considered.

The analysis of the DOSs of the trisubstituted compound $LaNi_{3.5}Al_{0.25}Mn_{0.5}Co_{0.75}$, plotted in Fig. 12, shows the relative positions of the main Ni d, Co d and Mn d peaks as a function of increasing energies. The Ni d states are much more strongly mixed with the Co d band than with the Mn d states. The relative intensities of the corresponding structures scale of course with the sample composition of the transition element. At the bottom of the valence band, below -6 eV, the Al s states provide a small but sizeable contribution. The main Co d peak is filled and the Fermi energy is rather found in the energy range spanned mostly by the Mn d states. The experimental valence band of $LaNi_{3.55}Al_{0.3}Mn_{0.4}Co_{0.75}$ shows in agreement with the DOSs calculations, a weak decrease of the intensity of the d peak and an increase of the contribution at -6 eV compared to the valence band of $LaNi_5$. These effects are less pronounced than in $LaNi_4Mn$ and $LaNi_4Al$, this may be related to the lower Mn and Al contents in the LaNi3S compound. The influence of Co is less visible since the experimental valence band of $LaNi_4Co$ is similar to that of $LaNi_5$. However, the results obtained from the XAS L_{II-III} edges of the Mn and Co transition metals can be related to the DOS calculations. The variations of the white line intensity at the Co and Mn edges have shown that the filling of the Co and Mn subbands is not the same in $LaNi_{3.55}Al_{0.3}Mn_{0.4}Co_{0.75}$ as in $LaNi_4Co$ and $LaNi_4Mn$. The decrease of the Co white line intensity indicates that the Co d band is more filled whereas the increase of the Mn white line intensity indicates that the Mn d band is less filled in the trisubstituted than in the single substituted compounds. Since the Co subband is located below the Mn subband, the Co d band is filled before the Mn subband. Thus the DOS results are consistent with the experimental XAS observation of a decrease in the contribution of the empty d states per Co atom, between $LaNi_4Co$ and the LaNi3S sample associated with an increase in the empty d states per Mn atom.

From the DOS calculations, it is remarkable to note that the estimated number of holes in the transition metal d bands, up to the valley which marks the rise of the La d states, is the same, four holes, for both the $LaNi_4Co$ and LaNi3S samples. In the hydride $LaNi_4CoH_4$,[18,29] the Fermi level falls just at the bottom of this valley, a factor that we correlated to the stability of this intermediate hydride. This corresponds to the existence of a first plateau pressure up to 4 H (f.u.)$^{-1}$, followed by an increase of the pressure, observed in the pressure composition isotherms.[8,9] The results of the DOS calculations indicate that a similar feature is expected to occur in the isotherms of the LaNi3S sample, for a H content of four per formula unit. In the LaNi3S compound, the particular position of the Fermi level relative to the location of the transition elements peaks leads to the formation of a stable hydride phase for an H content close to 4 H (f.u.)$^{-1}$. For higher H concentrations, the pressure is expected to rise. This corresponds to the experimentally observed β branch,[7] which plays an important role in the performance of the material in electrochemical applications.

VI Conclusions

This study has shown that there is a good correlation between experimental results and band structure calculations on $LaNi_4M$ intermetallic compounds. The main feature of the electronic structure of these materials is the presence of an additional 3d subband, whose position relative to the Ni d band depends on the nature of the d element. For Cu this subband is full and below the Fermi level, whereas for Mn, Fe and Co, the band is located above that of Ni and crosses the Fermi level. For the LaNi3S compound, the main effect is a change of the filling of the Mn and Co d bands compared to the single substituted compounds. The complete filling of the transition element d bands which corresponds to 4 H atoms per formula unit, both in $LaNi_4Co$ and LaNi3S, leads to stable hydrides up to that hydrogen concentration, in agreement with the existence of a plateau observed in the pressure composition isotherms up to 4 H (f.u.)$^{-1}$. The improvement in the cycle life of these electrode materials has been attributed to a weaker reduction of the size of the hydride grains (decrepitation process) which occurs in systems with a large hydrogen solid solution range (β branch) such as the one observed for LaNi3S above 4 H (f.u.)$^{-1}$. The breaking of the hydride grains into small particles leads to an increase of the surface, and therefore favors the corrosion process which occurs after several electrochemical cycles. Limiting the decrepitation leads therefore to a better cycle life. The correlation found in the present work between the electronic and thermodynamic properties appears to be important for a better understanding of the electrochemical performances of these electrode materials.

Acknowledgements

We are thankful to Mrs F. Briaucourt and Mrs F. Demany from the LCMTR (Thiais, France) for the preparation of the intermetallic compounds and to Mr F. Lecoester for his participation in the experiments at LURE. We would like to thank IDRIS (Institut de Developpement et Recherche en Informatique Scientifique) of CNRS (Centre National de la Recherche Scientifique) for providing the computing facilities for performing the electronic structure calculations.

References

1 A. Percheron-Guégan, J. C. Achard, J. Sarradin and G. Bronoël, *Electrode material based on lanthanum and nickel, electrochemical uses of such materials*, *Fr. Pat.* 75 161160, 1975; 77 23812, 1977; *US Pat.* 688537, 1978.
2 J. J. G. Willems, *Philips J. Res.*, 1984, **39**, (Suppl. 1).
3 J. J. G. Willems and K. H. J. Buschow, *J. Less Common Met.*, 1987, **129**, 13.
4 H. Ogawa, M. Ikoma, H. Kawano and I. Matsumoto, *J. Power Sources*, 1988, **12**, 393.
5 M. Ikoma, H. Kawano, I. Matsumoto and N. Yanagihara, *Eur. Pat. Appl.*, No. 0 271 043, 1987.
6 A. Percheron-Guégan, M. Latroche, J. C. Achard, Y. Chabre and J. Bouet, *Proceedings of the Symposium on Hydrogen and Metal Hydrogen Batteries*, ed. P. D. Bennet and T. Sakai, The Electrochemical Society, Pennington, NJ, 1994, vol. 94-27, p. 196.
7 M. Latroche, A. Percheron-Guégan, Y. Chabre, J. Bouet, J. Pannetier and E. Ressouche, *J. Alloys Compd.*, 1995, **231**, 537.
8 H. H. van Mal, K. H. J. Buschow and F. A. Kuijpers, *J. Less Common Met.*, 1973, **32**, 289.
9 M. Latroche, A. Percheron-Guégan and F. Bourée-Vigneron, *J. Alloys Compd.*, 1998, **265**, 209.
10 M. Gupta and L. Schlapbach, *Electronic properties in Hydrogen in Intermetallic Compounds I*, ed. L. Schlapbach, Springer-Verlag, 1988, vol. 63, p. 139 and references therein.
11 K. A. Geschneidner, Jr., T. Takeshita, Y. Chung and O. D. McMasters, *J. Phys. F*, 1982, **12**, L1.
12 H. Züchner, J. Kintrup, R. Dobrileit and I. Untiedt, *J. Alloys Compd.*, 1999, **293-295**, 202.
13 D. A. Tryk, In Tae Bae, Y. Hu, S. Kim, M. R. Antonio and D. A. Scherson, *J. Electrochem. Soc.*, 1995, **142**, 824.
14 D. A. Tryk, In Tae Bae, D. A. Scherson, M. R. Antonio, G. W. Jordan and E. L. Huston, *J. Electrochem. Soc.*, 1995, **142**, L76.
15 S. Mukerjee, J. Mc Breen, J. J. Reilly, J. R. Johnson, G. Adgik, K. Petrov, M. P. S. Kumar, W. Zhang and S. Srinivasan, *J. Electrochem. Soc.*, 1995, **142**, 2278.
16 H. H. Hsieh, Y. K. Chang, W. F. Pong, J. Y. Pieh, P. K. Tseng, T. K. Sham, I. Coulthard, J. Naftel, J. F. Lee, S. C. Chung and K. L. Tsang, *Phys. Rev. B*, 1998, **57**, 15204.
17 A. Slebarski, A. Jezierski, S. Mähl, M. Neumann and G. Borstel, *Phys. Rev. B*, 1997, **56**, 7245.
18 M. Gupta, *J. Alloys Compd.*, 1999, **293–295**, 190.
19 A. Percheron-Guégan, C. Lartigue, J.-C. Achard, P. Germi and F. Tasset, *J. Less-Common Met.*, 1980, **74**, 1.
20 U. von Barth and L. Hedin, *J. Phys. C*, 1972, **5**, 1629.
21 O. K. Andersen, *Phys. Rev. B*, 1975, **3060**, 12.
22 G. Lehman and M. Taut, *Phys. Status Solidi (b)*, 1972, **54**, 469.
23 K. Yvon and P. Fisher, in *Hydrogen in intermetallic compounds I*, ed. L. Schlappbach, *Top. Appl. Phys.*, vol. 63, Springer Verlag, 1988, p. 87.
24 A. Percheron-Guégan, in *Interstitial Intermetallic Alloys*, ed. F. Grandjean, Kluwer Academic Publishers, The Netherlands, 1995, p. 77.
25 J. Fink, Th. Müller-Heinzerling, B. Sherrer, W. Speier, F. U. Hillebrecht, J. C. Fuggle, J. Zaanen and G. A. Sawatzky, *Phys. Rev. B*, 1985, **32**, 4899.
26 W. E. Wallace, *J. Less-Common Met.*, 1982, **88**, 141.
27 M. Weinelt, A. Nilsson, T. Wiell, P. Bennich, O. Karis, N. Wassdahl, J. Stöhr and M. G. Samant, *Phys. Rev. Lett.*, 1997, **78**, 967.
28 J. C. Fuggle, F. Hillebrecht, R. Zeller, Z. Zolnierek, P. A. Bennet and Ch. Freiburg, *Phys. Rev. B*, 1982, **27**, 2145.
29 E. Gurewitz, H. Pinto, M. P. Dariel and H. Shaked, *J. Phys. F: Met. Phys.*, 1983, **13**, 545.